Published on 16 February 2016. Downloaded by Nanyang Technological University on 15/03/2016 09:34:37.

CrystEngComm

PAPER

View Article Online
View Journal | View Issue

CrossMark
click for updates

Cite this: *CrystEngComm*, 2016, **18**, 2072

Bulk growth, crystalline perfection and optical characteristics of inversely soluble lithium sulfate monohydrate single crystals grown by the conventional solvent evaporation and modified Sankaranarayanan–Ramasamy method

A. Silambarasan,[a] E. Nageswara Rao,[b] S. Venugopal Rao,[b] P. Rajesh*[a] and P. Ramasamy[a]

Received 2nd January 2016,
Accepted 8th February 2016

DOI: 10.1039/c6ce00012f

www.rsc.org/crystengcomm

Good quality bulk size single crystals of inverse soluble lithium sulphate monohydrate (LSMH) have been grown by the modified Sankaranarayanan–Ramasamy (SR) method. A growth rate as high as 3 mm per day has been obtained for LSMH growth without substantially degrading the optical quality. The rocking curve recorded using the high resolution X-ray diffraction (HRXRD) technique reveals that the crystals grown by this method have a high degree of crystalline perfection. The optical quality of the crystals was studied using an UV-vis-NIR spectrum and the optical constants of the LSMH crystals were calculated. The laser damage threshold value of the grown crystals has been determined using a nanosecond Nd:YAG laser operating at 532 nm. Photoconductivity studies of the grown LSMH crystals reveal a positive photoconductivity behaviour of the grown crystals. The photoluminescence spectrum of the LSMH crystals shows a prominent emission peak at 373 nm. The third order non-linear optical properties of the LSMH crystals were investigated in detail by the Z-scan technique using a He–Ne laser operating at 632.8 nm. The non-linear refractive index (n_2), non-linear absorption coefficient (β) and third order non-linear susceptibility ($\chi^{(3)}$) of the LSMH crystals were calculated.

1. Introduction

The pursuit for efficient non-linear optical materials is intensely devoted to in various fields of optoelectronic and photonic device applications such as frequency conversion, ultra-compact lasers, optical switching, optical modulators, optical communication, optical limiting and optical data processing. In this context, an extensive search is being carried out into non-linear optical (NLO) materials with a high non-linear response, wide transparency range, better laser damage resistance, high mechanical stability and ease in fabrication as compared to other inorganic counterparts.[1–3] Lithium sulphate monohydrate ($Li_2SO_4 \cdot H_2O$) (LSMH) is one such good non-linear optical material and also has piezoelectric and pyroelectric properties.[4–7] LSMH comes under the monoclinic non-ferroelectric polar point group 2 (C_2). The lattice parameters of LSMH are a = 5.449 Å, b = 4.832 Å and c = 8.137 Å.[8,9] The piezoelectric and elastic coefficients of LSMH and the temperature coefficients have been reported.[7,10] The materials with a compound of LSMH such as lithium sulfate monohydrate oxalate, glycine lithium sulfate, EDTA and Cu(II)-added LSMH show a higher NLO activity.[11–14] LSMH has also proven to be an interesting host for luminescence and thermo-luminescence for dosimetry applications.[15,16] Bohaty *et al.*[17] demonstrated LSMH as a promising non-linear medium for up and down Raman laser frequency converters. Despite these properties, the grown LSMH crystals had some defects and the transparency was poor.[5,6] The inclusions play a crucial role in the quality of the crystals. Inverse (negative) solubility, pyroelectric behaviour and higher density (2.06 g cm^{-3}) of the saturated LSMH solution make the crystal growth more difficult than that of other materials during its growth processes. The inverse solubility behaviour and nucleation curve of LSMH single crystals have been reported by us recently.[18]

The growth of bulk size crystals with orientation control is of importance for crystal growers. It is required to grow crystals with exceptional quality by optimization of the crystal growth method and materials conveniently. In the crystal growth literature, different solution growth methods

[a] *Center for Crystal Growth, Department of Physics, SSN College of Engineering, Kalavakkam 603110, Tamilnadu, India. E-mail: rajeshp@ssn.edu.in, rajeshppraj@gmail.com; Fax: +91 44 27475166; Tel: +91 9840522490*
[b] *Advanced Centre of Research in High Energy Materials (ACRHEM), University of Hyderabad, 500046, Telangana, India*

 This journal is © The Royal Society of Chemistry 2016

Published on 16 February 2016. Downloaded by Nanyang Technological University on 15/03/2016 09:34:37.

including the solvent evaporation method,[19,20] low temperature hydrothermal method[21] and uniaxial solution crystallization Sankaranarayanan–Ramasamy (SR) method[22] have been applied to grow bulk size hydrous crystals. The SR method is a suitable method to grow healthy, defect-free, high transparency bulk crystals from solution in a chosen orientation.[22–24] In the SR method the free convection flows are driven within the solution (inside of the ampoule) itself by keeping a different temperature at the top and bottom portion of the solution growth systems. Although Boopathi *et al.*[5] grew LSMH crystals by this method, the growth rate and crystal size are much less due to the spurious nucleation at the top region of the solution. By considering these facts, we recently demonstrated significant modifications in the SR method to grow bulk size LSMH single crystals with a higher growth rate.[25] In this paper, we report the schematic representation of the modified SR method to grow bulk size inverse soluble LSMH single crystals in addition to their specific features of the instrumental process. The crystalline perfection of the grown LSMH crystals was studied by recording the rocking curve widths using high resolution X-ray diffraction (HRXRD). A systematic investigation on UV-vis-NIR transmittance, the laser damage threshold (LDT) and the photoluminescence properties of LSMH single crystals has been carried out to evaluate the optical behaviour of the LSMH single crystals. To our knowledge, the photoconductivity behaviour and the third order optical non-linearity and optical limiting properties of the LSMH single crystals have not been reported. In this context, this work also investigates the photoconductivity behaviour and third order non-linear optical properties of the grown LSMH single crystals.

2. Experimental section

Materials and methods

The inverse solubility and metastable zone width of LSMH have been discussed in our recent paper.[18] It is found that the concentration of solute in the aqueous solution decreases with increasing temperature because of the inverted solubility behaviour of LSMH. The solubility of LSMH was found to be 32.81 g per 100 ml at 40 °C. The modified SR method was employed to grow <010> directed bulk size LSMH single crystals. In order to avoid the problems due to the negative solubility behaviour and higher density of the solution leading to spurious nucleation during growth, we introduced the inverted temperature gradient and cone-type ampoule. Hence, the top and bottom portions of the setup have been kept in a lower and higher temperature environment, respectively. In addition, the lower temperature at the top of the ampoule is maintained to be above room temperature to avoid the spurious nucleation at the surface of the solution. As this free convective flow leads to initiation of the crystallization from the mounted seed, the single crystals start to grow. This convective flow of the solution leads to the inclusion being stopped during crystal growth. An uncomplicated growth apparatus of the modified SR method made up of a glass container of size 30 × 30 × 30 cm^3 and an ampoule of inner diameter 20 mm using two controllable ring heaters is shown in Fig. 1.

Initially, the crystals of LSMH were grown by the conventional solvent evaporation method (slow evaporation solution growth technique). The commercially available lithium sulfate monohydrate purchased from SRL chemicals (>99% purity) was used for growth after repeated recrystallization. A saturated solution at 40 °C of the compound was prepared using water as the solvent and the temperature of the solution was increased while stirring the solution in order to have high homogeneity. The solution was filtered to remove any impurities present and the beaker containing the saturated solution was covered with perforated polythene paper. Consecutively, to maintain a constant 40 °C temperature of the solution, it was carefully kept undisturbed in the constant temperature water bath. In the span of 25 days LSMH single crystals of a maximum dimension of 15 × 10 × 4 mm^3 have been grown. The crystals grown by the conventional solvent evaporation method are shown in Fig. 2(a). Among the grown crystals, some have inclusions and are visually of low optical quality. However, we have chosen the visually best crystals for further studies. Based on the quality of the crystals grown by the conventional solvent evaporation method, a suitable seed crystal having a size 4 × 4 × 3 mm^3 with <010> (y-direction) was selected for unidirectional crystal growth. To enforce growth along the <010> direction the chosen <010> directed crystal was mounted in the bottom of the ampoule without polishing the surface. Now, the ampoule was kept in the glass water bath to maintain a constant ambient temperature. A filtered supersaturated solution is carefully poured into the growth ampoule without disturbing the position of the seed crystal. As discussed above, the growth was initiated with a suitable temperature provided by the ring heater at the top region of the saturated solution. The temperature around the top and bottom of the ampoule is maintained at 38 °C and 40 °C respectively. Under this optimized condition

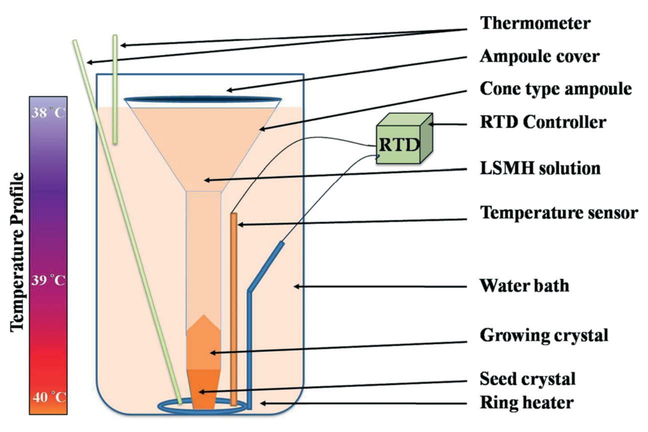

Fig. 1 Schematic diagram of the modified SR method experimental setup to grow inverted solubility LSMH single crystals.

Published on 16 February 2016. Downloaded by Nanyang Technological University on 15/03/2016 09:34:37.

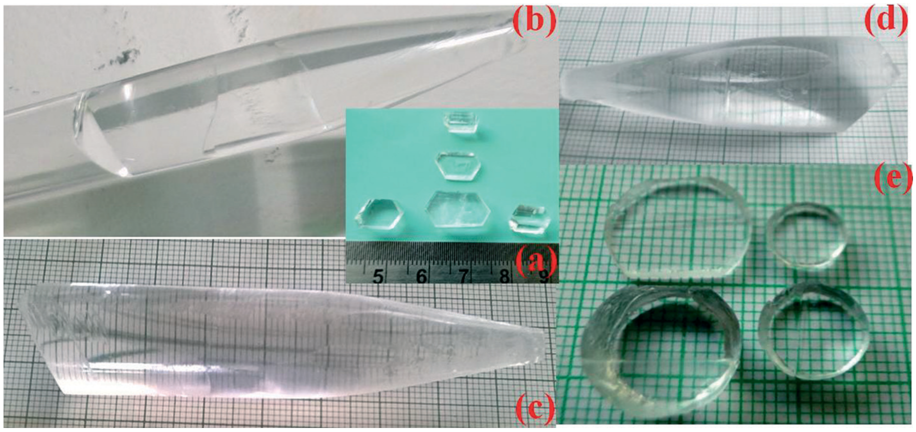

Fig. 2 (a) Conventional method grown crystals. (b) <010> directed crystal grown by the SR method with the ampoule. (c and d) Detached SR grown crystals. (e) Cut and polished LSMH ingots (cut from crystal (d)).

highly transparent crystal growth was seen after a week. After 30 days of the growth period, a good quality crystal was harvested with a maximum size of 20 mm in diameter and 80 mm in length. The average growth rate along the <010> direction was 3 mm per day which is very high as compared to that of LSMH crystals obtained from the conventional SR method.[5] Finally, the ampoule was detached from the growth system and the grown crystal is carefully removed from the ampoule using a diamond glass cutter. Fig. 2(b) shows the grown <010> directed LSMH crystal with the ampoule by the SR method. The authors grew three crystals by this method. Two of them are shown in Fig. 2(c) and (d). The cut and polished ingots (Fig. 2(e)) are sliced from the crystal Fig. 2(d). The same has been used for all the characterizations in the present work.

3. Characterization techniques

The degree of crystalline perfection of the LSMH crystals was assessed using a PANalytical X'pert PRO MRD high resolution XRD system. The well collimated and monochromatic CuKα_1 (λ = 1.54056 Å) beam obtained from the four bounce monochromator Ge (220) crystals has been used as the exploring X-ray beam. The rocking curves of the crystals for the (011) diffraction planes were recorded in symmetrical Bragg geometry using natural facets by performing an omega scan. The diffracted intensity from the specimen was detected using a scintillation detector. The optical transmittance of the grown LSMH crystals was recorded from UV to NIR in the wavelength range of 200–1100 nm using a Perkin Elmer UV-vis-NIR spectrophotometer at room temperature. The thickness of the samples (both conventional and SR grown crystals) used for measurement was 2 mm. A Q-switched Nd:YAG laser of pulse width 7 ns and 10 Hz repetition rate was used for laser damage studies (LDT). <010> directed grown LSMH samples identical in thickness and surface finish (polishing) were kept 1 cm above the focus point of the laser for the measurements. The energy of the 532 nm laser radiation was attenuated using appropriate neutral density filters and was measured using an energy power meter. The nanosecond laser was focused by a convex lens of 100 mm focal length. The photoconductivity of the crystal was studied using a Hind high vacuum cryostat facility instrument at room temperature. Electrical contacts were made at a spacing of about 0.3 cm on the polished crystal samples using silver paste. The DC input was increased from 1 to 50 volts in steps and the corresponding dark currents and photocurrents were noted from the electrometer. The *I–V* curve was first measured in the dark, then under illumination. Photoconductivity measurements were carried out on a polished portion of the grown single crystal by fixing it onto a glass slide in a vacuum chamber. The electrical contacts of the sample were made by copper clips fixed onto the crystal at 0.3 cm spacing using silver paint and the sample was connected in series with a DC power supply and KEITHLEY 485 picoammeter of the instrument. The sample was illuminated with a full spectrum of the xenon lamp (50 W) and the corresponding photocurrent was recorded for the applied voltage. In order to know the luminescent behavior of LSMH, the PL spectrum was recorded using a Shimadzu spectrofluorometer (RF-5301PC, Japan) at room temperature with a 150 W high pressure xenon lamp as the excitation source which encloses a photomultiplier tube at the detector side. The emission spectra were recorded using a spectral slit width of 3 nm. Z-scan measurements were carried out for the conventional and SR grown LSMH crystals using a continuous wave He–Ne laser (5 mW) of 632.8 nm with a peak intensity of 25.5 MW m^{-2}. The single beam of the laser source is allowed to pass through a Gaussian filter to have a Gaussian beam. This beam is focused using a lens of focal length 30 mm into the sample and the beam waist was estimated to be 3.3 mm at the focus. The measurements are carried out on the <010> direction samples having a thickness of 0.52 mm. The sample was moved along the travelling *Z*-direction at the focal point and the transmittance was recorded at a finite aperture in the far field as a function of the sample position.

 This journal is © The Royal Society of Chemistry 2016

Published on 16 February 2016. Downloaded by Nanyang Technological University on 15/03/2016 09:34:37.

4. Results and discussion

4.1. HRXRD studies

Crystalline perfection of the grown crystals plays an important role in their device performance which depends on the growth techniques/conditions. In order to check the crystalline quality of the LSMH single crystals grown by this method, a high resolution X-ray diffraction (HRXRD) study was employed. A HRXRD diffraction spectrum taken from the (011) diffracting planes of the LSMH samples is shown in Fig. 3. The measured FWHM value of the diffraction curve of LSMH is 9.8 arc s, which is very close to that expected from the plane wave theory of dynamical X-ray diffraction.[26] This low FWHM of the rocking curve (RC) testifies that there are no structural distortions and low/very low angle grain boundaries in the crystal. The curve is quite sharp with a good symmetry with respect to the exact Bragg peak position (taken as zero for the sake of convenience). This confirms that the grown crystal has much fewer vacancies and interstitial defects in its atomic substitutional positions.[27] Although the X-ray diffraction of the different diffracting planes of a crystal have a different RC and FWHM, the observed FWHM of 8 arc s of the diffraction plane of (100) for the crystal grown by the conventional SR method[5] is comparable with the quality of the present study where the FWHM is 9.8 arc s of the (011) diffracting plane for the crystal grown by the modified SR method. It is also interesting to note that this much crystalline perfection of LSMH is observed, even though the crystals are grown with a higher growth rate by the modified SR method. This could be possibly because the crystals grown by this method allowed homogenous solution flow rates during growth which leads to inclusion-free crystals and a perfect molecular arrangement in the lattice.

4.2. Optical transmittance

Fig. 4 shows the recorded optical transmittance spectra of the conventional solvent evaporation and modified SR method grown crystals in which the characteristic absorption band of the LSMH crystals occurs below 200 nm. From the spectra, it is observed that the SR grown crystals have higher transparency than the conventional grown crystals. The ~80% transmittance in the visible and NIR region of the SR grown crystals reveals good optical quality of the grown crystals. An increase in transmittance throughout the visible and NIR region represents the good optical homogeneity of the material which is due to excellent crystalline perfection of the grown LSMH single crystals as seen in the HRXRD studies. This high optical transmittance spectrum of the crystals is a primary requirement for many optical applications. The refractive index and bandgap of the material were calculated from the transmittance spectra.[28–30] The measured transmittance T was used to calculate the absorption coefficient α using the formula:

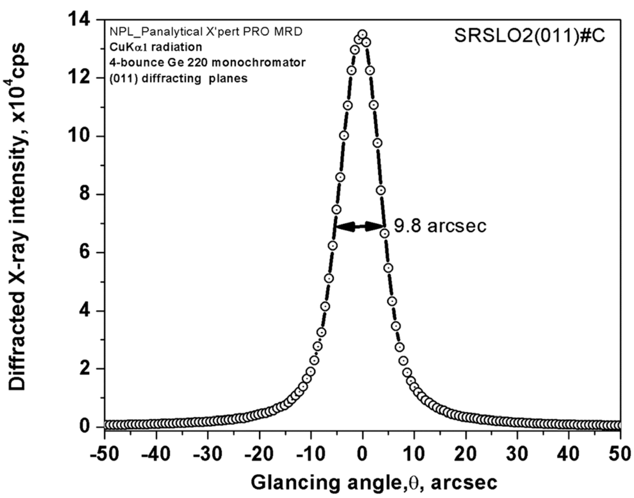

Fig. 3 HRXRD spectrum of the grown LSMH crystal.

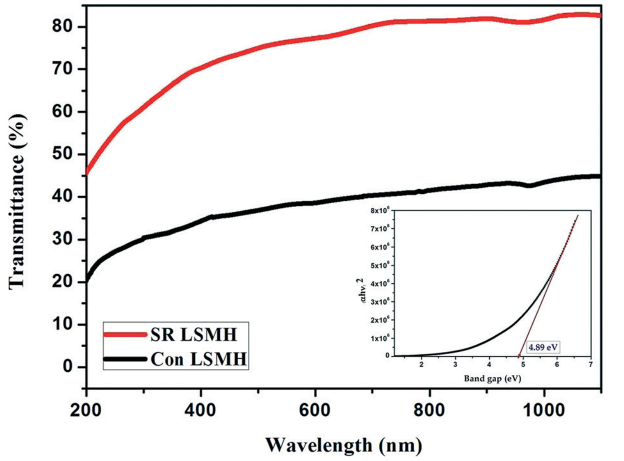

Fig. 4 Transmittance spectra of the conventional and SR method grown LSMH crystals and the corresponding Tauc plot.

$$\alpha = \frac{2.303\log\left(\frac{1}{T}\right)}{t} \quad (1)$$

where T is the transmittance and t is the thickness of the sample. A similar absorption coefficient was calculated for the transmitted spectra recorded from different locations of the grown crystal.

The reflectance R in terms of the absorption coefficient α and refractive index n can be derived from the relations:

$$R = \frac{\exp(-\alpha t) + \sqrt{\exp(-\alpha t)T - \exp(-3\alpha t)T + \exp(-2\alpha t)T^2}}{\exp(-\alpha t) + \exp(-2\alpha t)T} \quad (2)$$

and

$$n = \frac{-(R+1) - \left(2\sqrt{R}\right)}{(R-1)} \quad (3)$$

The value of the refractive index at 2.33 eV is found to be 1.72. The optical bandgap estimated from the optical

Published on 16 February 2016. Downloaded by Nanyang Technological University on 15/03/2016 09:34:37.

absorption coefficient α near the absorption edge for the direct transition is given by

$$(\alpha h\nu)^2 = A(E_g - h\nu) \tag{4}$$

where A is a constant, E_g is the optical bandgap, h is Planck's constant and ν is the frequency of incident photons. The optical bandgap was evaluated by plotting $(\alpha h\nu)^2$ *vs.* $h\nu$ as shown in the inset of Fig. 4 and extrapolating the linear portion of the absorption edge $(\alpha h\nu)^2$ in the photon energy axis gives the optical bandgap of the crystal. The approximate optical bandgap value of the LSMH single crystal is found to be 4.89 eV.

4.3. Surface laser damage analysis

Investigation of crystal stability against intense nanosecond/picosecond laser pulses is one of the most important prerequisites for applications in optoelectronic devices. A schematic representation of the experimental setup used in this study is shown in Fig. 5. Since tiny scratches or a little contamination on the surface of the sample can substantially lower the surface damage threshold, the LSMH crystal sample was well polished using its diluted mother (LSMH) solution and alumina powder to avoid defects, impurities and imperfections on the surface. The higher transmission behavior and lower reflectance of the crystal proves that the laser-induced damage on the crystal surface is always on the bottom side of the crystal. Initially ~15 mJ energy was applied on the conventional grown crystals and no damage was observed up to 30 s. When it is increased to ~20 mJ a small spot (~0.5 mm) appeared on the surface of the sample. When it was further increased to ~30 mJ for 10 s, a crack appeared. The same experimental arrangement was used to measure the LDT of the crystals grown from the SR technique and it was observed that the crystals could withstand up to ~25 mJ and no damage was noticed even after 20 s of exposure. When the laser energy increased to ~29 mJ, a small spot appeared on the surface of the crystal after 20 s. When the experiment was repeated with the energy increased to 47 mJ, the surface of the crystal cracked just after 10 s. Care was taken to select a fresh region after each shot to avoid cumulative effects resulting from multiple exposure. Microscopic images of the conventional and SR method grown crystals are shown in Fig. 6(a) and (b), respectively. The surface damage threshold of the crystal was calculated using the expression:[31]

power density

$$P_d = \frac{E}{\pi r^2 \tau} \tag{5}$$

where E is the laser energy (mJ), r is the radius of the beam spot (cm) and τ is the pulse width of the 532 nm ns laser. The calculated values of the laser damage threshold after a single shot and multiple shots are provided in Table 1. It is known that the material with a higher specific heat is more resistant to laser damage. Also, laser-induced bulk damage may occur due to many intrinsic factors arising from the optical behavior of the materials and extrinsic factors such as material defects, impurities and surface roughness of the materials.[32] The results prove that the LDT value of the crystals obtained from the SR method is higher than that of the conventionally grown crystals because of the higher crystalline perfection.

4.4. Photoconductivity measurement

Photoconductivity is an important study for solids, and is especially apparent for semiconductors and insulators, and so it is used to investigate the structure and electronic properties of the material. Photoconduction is a function of temperature, applied field, intensity of light and energy of radiation of the crystal. When the material is illuminated with photons of an energy (E) greater than its bandgap energy (E_g), electron–hole pairs are generated and the conductivity of the material increases. Fig. 7 shows the measured variations of photocurrent (I_p) and dark current (I_d) with applied field for the samples at room temperature. Both the photo and dark currents of the LSMH crystal increase linearly with applied field. It is observed from the plot that at any instant of applied field the photocurrent is greater than the dark current, thus suggesting that the conventional and SR grown LSMH

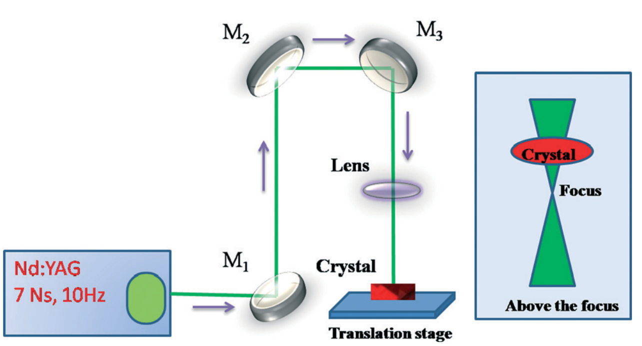

Fig. 5 Schematic diagram of the experimental setup to measure the LDT.

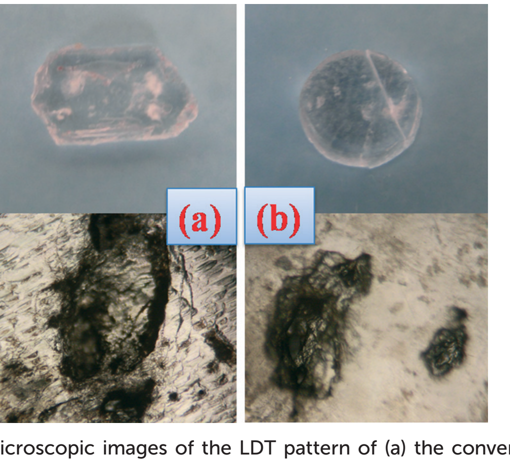

Fig. 6 Microscopic images of the LDT pattern of (a) the conventional and (b) the SR method grown crystal and the test crystal samples.

 This journal is © The Royal Society of Chemistry 2016

Published on 16 February 2016. Downloaded by Nanyang Technological University on 15/03/2016 09:34:37.

Table 1 Laser damage threshold (LDT) values of the LSMH crystals

Sample	Single shot		Multiple shot (10 Hz)	
	Energy (mJ)	LDT value (GW cm^{-2})	Energy (mJ)	LDT value (GW cm^{-2})
Conventional	75.5	25.99	20 (20 s)	6.88
SR	130	44.75	29 (20 s)	9.9

exhibits positive photoconductivity. This positive photoconductivity behavior can be attributed to the generation of mobile charge carriers caused by the absorption of photons. The increase in the number of charge carriers or their lifetime in the presence of radiation is also responsible for the positive photoconductivity. The high value of photocurrent of the crystals grown from the SR method is due to the absence of vacancies and interstitial defects as evidenced by HRXRD and the lack of traps and the population of the intrinsic centre formed by direct excitation of charge carriers in the crystal. Also, the increase in the transmittance percentage due to higher optical homogeneity is attributed to the enhancement in photoconductivity of the SR grown crystals. This positive photoconductivity and wide bandgap of LSMH can be applied towards soliton wave communication applications.[33]

4.5. Luminescence studies

Photoluminescence spectral analysis is one of the effective tools to provide relatively direct information about the physical properties of materials at the molecular level, including shallow and deep level defects and gap states. In order to identify the photoluminescence characteristics of LSMH, the grown crystals were excited at 250 nm. The emission spectra are recorded at room temperature in the range of 340–400 nm and is shown in Fig. 8. LSMH single crystals show an emission peak at 373 nm. But the intensity of the peak depends upon the crystallinity. The intensity of the emission peak (out-coming light) depends on the intrinsic defect concentration as well as the transparency of the crystal. The SR grown crystal has higher transparency which facilitates higher light emission.

4.6 Z-scan measurements

For the usage of the crystals to be efficient, it is necessary to have quantitative information about their non-linear optical properties. The Z-scan measurement using a single Gaussian beam in tight focus geometry is a standard technique to determine the magnitude and sign of the non-linear change in the index and the changes in the absorption coefficient of a material.[34–36] The rapid acceptance of this technique is due to the simplicity in instrumental manipulation and interpretation of the data. The measured normalized transmittance of the closed aperture and open aperture of the Z-scan studies is used to calculate various non-linear optical parameters. The normalized transmittance of the open aperture Z-scan measurement for the LSMH crystals grown from the conventional and SR method is illustrated in Fig. 9(a). The maximal transmission at the focus ($Z = 0$) is indicative of the saturation of absorption at high intensity. From the open aperture Z-scan spectrum (Fig. 9(a)), the non-linear refractive index of absorption is calculated by the relation:[34]

$$\beta = \frac{2\sqrt{2}\Delta T}{I_O L_{\text{eff}}} \tag{6}$$

where ΔT is the one valley value at the open aperture Z-scan curve, $L_{\text{eff}} = \frac{1-\exp(-\alpha L)}{\alpha}$ is the effective thickness of the

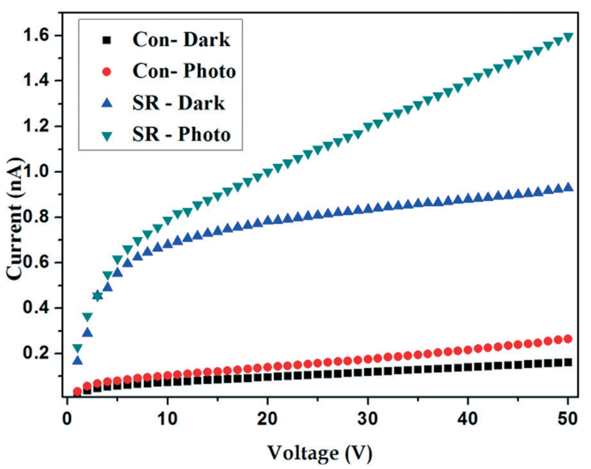

Fig. 7 Photoconductivity of the conventional and SR method grown LSMH crystals.

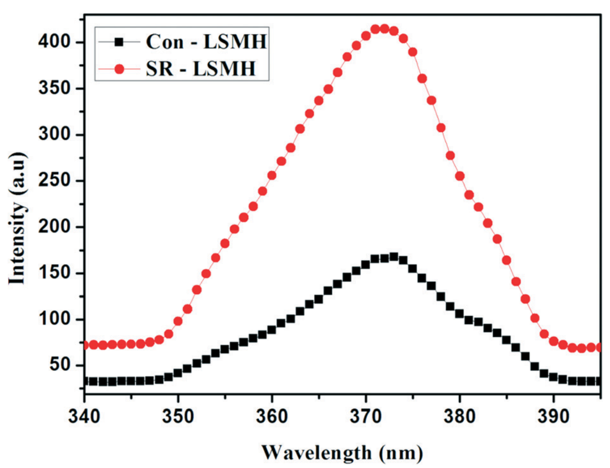

Fig. 8 Photoluminescence spectra of the conventional and SR method grown LSMH crystals.

Published on 16 February 2016. Downloaded by Nanyang Technological University on 15/03/2016 09:34:37.

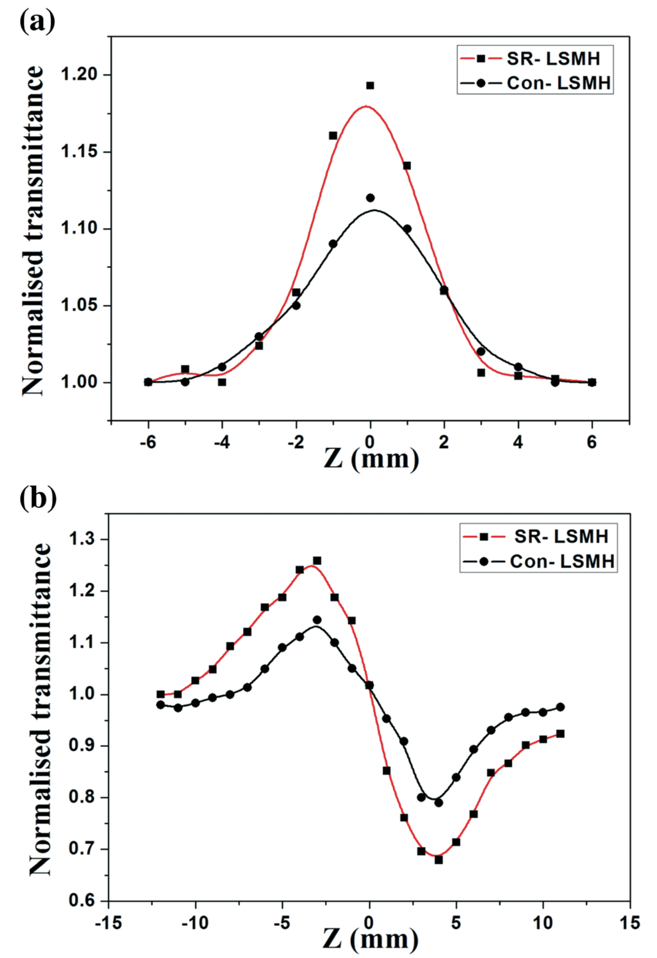

Fig. 9 (a) Open aperture Z-scan spectra of the conventional and SR method grown LSMH crystals. (b) Closed aperture Z-scan spectra of the conventional and SR method grown LSMH crystals.

sample, α is the linear absorption coefficient of the sample, L is the thickness of the sample (0.52 mm) and I_o is the intensity of the laser at the focus (25 MW m^{-2}).

The transmittance for the closed aperture Z-scan for the LSMH crystals grown from the conventional and SR method is measured as a function of sample position with the aperture placed at the far field and it is shown in Fig. 9(b). The pre-focal peak to the post-focal valley configuration of the closed aperture Z-scan spectrum of LSMH clearly shows that the sign of the non-linear refractive index is negative.[35] In order to find the non-linear refractive index of LSMH, the on-axis phase shift

$$|\Delta\Phi|$$

can be calculated from the relation:[34,36]

$$|\Delta\Phi| = \frac{\Delta T_{p-v}}{0.406(1-S)^{0.25}} \tag{7}$$

where $S = 1 - \exp\left(\frac{-2r_a^2}{w_a^2}\right)$ is the linear transmittance of the aperture radius r_a and the beam radius at aperture Ω_a. Hence, the third order non-linear refractive index n_2 was evaluated using the following relation:

$$n_2 = \frac{\Delta\Phi}{kI_O L_{\text{eff}}} \tag{8}$$

where $k = \frac{2\pi}{\lambda}$, and λ is the wavelength of the laser. The real and imaginary parts of the third order non-linear optical susceptibility were determined using the values of β and n_2 by the relations:[34,36]

$$\operatorname{Re}\chi^{(3)}(\text{esu}) = 10^{-4}\frac{\left(\varepsilon_O C^2 n_O^2 n_2\right)}{\pi}\left(\frac{\text{cm}^2}{\text{W}}\right) \tag{9}$$

and

$$\operatorname{Im}\chi^{(3)}(\text{esu}) = 10^{-2}\frac{\left(\varepsilon_O C^2 n_O^2 \lambda\beta\right)}{4\pi^2}\left(\frac{\text{cm}}{\text{W}}\right) \tag{10}$$

where ε_o is the permittivity of a vacuum, C is the velocity of light in a vacuum, and n_o is the linear refractive index of the sample. The absolute value of $\chi^{(3)}$ was obtained from the following relation:

$$|\chi^{(3)}| = [(\text{Re}\chi^{(3)})^2 + (\text{Im}\chi^{(3)})^2]^{0.5} \tag{11}$$

The estimated third order non-linear properties of the LSMH crystals grown from the conventional and SR method are summarized in Table 2. The value of the non-linear absorption coefficient (β) of LSMH estimated from the open aperture Z-scan curve is in the order of 10^{-4} m W^{-1} and the non-linear refractive index (n_2) calculated from the closed aperture Z-scan curve is in the order of 10^{-11} m^2 W^{-1}. In contrast with the conventionally grown crystals, the SR grown crystals exhibited larger non-linear transmittance values with the same input intensity towards the focus leading to the slight variation in the estimated parameters and indicating an enhanced light–matter interaction (non-linearity).[37] The slightly enhanced non-linear refractive index (n_2) can be attributed to the superior quality of the crystals grown with the SR method. The negative sign of the non-linear refractive index indicates the self-defocusing nature of the material and this is attributed to variation of the refractive index with temperature resulting from absorption of radiation at 632.8 nm.[35] The self-defocusing behavior of LSMH may have an advantage in practical devices, by providing a self-protecting mechanism for the limiter in optical systems such as direct viewing devices (telescopes, gunsights, *etc.*) and night vision devices.[38,39]

5. Conclusions

In view of the estimated advantages, the SR method was improved to grow inverse solubility large LSMH single crystals. The method enhanced the free convective flow within the

 This journal is © The Royal Society of Chemistry 2016

Published on 16 February 2016. Downloaded by Nanyang Technological University on 15/03/2016 09:34:37.

Table 2 Measured Z-scan parameters of LSMH of a He–Ne laser at a wavelength of 632.8 nm

Parameters	Conventional	SR method
Effective thickness (L_{eff}) (m)	4.6×10^{-4}	5.0×10^{-4}
Aperture linear transmittance (S)	0.52	0.52
Non-linear refractive index (n_2) ($m^2 W^{-1}$)	-0.9×10^{-11}	-1.3×10^{-11}
Non-linear absorption coefficient (β) ($m W^{-1}$)	2.6×10^{-4}	2.5×10^{-4}
Real part of the third order non-linear susceptibility (Re χ^3) (e.s.u.)	-4.8×10^{-10}	-7.2×10^{-10}
Imaginary part of the third order non-linear susceptibility (Imχ^3) (e.s.u.)	4.9×10^{-8}	4.8×10^{-8}
Third order non-linear susceptibility (χ^3) (e.s.u.)	4.9×10^{-8}	4.8×10^{-8}

mother solution of LSMH during growth, which markedly increases the crystal growth rate. The crystalline perfection of the grown crystals by the modified SR method is revealed by HRXRD studies. The LSMH crystals grown by the modified SR method had higher transmittance and higher laser stability than the crystals grown by the conventional method. The intense violet luminescence and positive photoconductivity of the SR grown LSMH crystals were observed. From the Z-scan measurement, the non-linear refractive index n_2, non-linear absorption coefficient β and third order non-linear susceptibility $\chi^{(3)}$ of the LSMH crystals are calculated. In contrast with the conventionally grown crystals, the SR grown crystals exhibited larger non-linear transmittance values with the same input intensity. The negative sign of the non-linear refractive index of LSMH indicates the self-defocusing behavior of the material, which is an essential property for its application in the protection of optical sensors. Hence, the LSMH crystals grown by this method fulfilled all the requirements, such as having a good non-linear response and splendid crystal characteristics including higher laser damage stability, superior optical quality and large crystal size with desired facets and controllable crystal thickness. The present crystallization process of LSMH by the modified SR method exemplified here can be used as a model to grow other such inversely soluble materials.

Acknowledgements

The authors gratefully acknowledge DAE-BRNS, Government of India for the financial support (Ref: no.2012/34/52/BRNS/2037). The authors thank Dr. A. K. Karnal, Crystal Growth Laboratory, LMDDD, Raja Ramanna Centre for Advanced Technology, Indore for his fruitful discussions. They sincerely thank Dr. K. K. Maurya, NPL, Council of Scientific and Industrial Research, New Delhi for HRXRD measurements. The authors are also thankful to Dr. S. Kalainathan, School of Advanced Sciences, VIT University, Vellore for extending Z-scan facilities.

References

1 N. Zaitseva, L. Carman and I. Smolsky, *J. Cryst. Growth*, 2002, **241**, 363.
2 M. D. Aggarwal, J. Stephens, A. K. Batra and R. B. Lal, *J. Optoelectron. Adv. Mater.*, 2003, **5**, 555.
3 H. P. Wu, S. L. Pan, H. W. Yu, D. Z. Jia, A. M. Chang, H. Y. Li, F. F. Zhang and X. Huang, *CrystEngComm*, 2012, **14**, 799.
4 L. Bayarajargal, *Cryst. Res. Technol.*, 2008, **43**(11), 1138.
5 K. Boopathi, P. Rajesh and P. Ramasamy, *J. Cryst. Growth*, 2012, **345**, 1.
6 R. Priya, S. Krishnan, C. Justin Raj and S. Jerome Das, *Cryst. Res. Technol.*, 2009, **44**(12), 1272.
7 R. Bechmann, *Proc. Phys. Soc., London, Sect. B*, 1952, **65**, 375.
8 S. B. Lang, *Phys. Rev. B: Solid State*, 1971, **4**, 3603.
9 M. V. Hobden, *J. Appl. Phys.*, 1967, **38**, 4365.
10 W. P. Mason, *Piezoelectric crystals and their application to ultrasonics*, Van Nostrand, New York, 1950.
11 H. Yadav, N. Sinha and B. Kumar, *Mater. Res. Bull.*, 2015, **64**, 194.
12 M. R. Suresh Kumar, H. J. Ravindra and S. M. Dharmaprakash, *J. Cryst. Growth*, 2007, **306**, 361.
13 R. Manimekalai, A. P. Raj and C. R. Raja, *Opt. Photonics J.*, 2012, **2**, 216.
14 K. Boopathi, P. Ramasamy and G. Bhagavannarayana, *J. Cryst. Growth*, 2014, **386**, 32.
15 S. V. Upadeo and S. V. Moharil, *Radiat. Eff. Defects Solids*, 1996, **138**, 167.
16 S. P. Puppalwar, S. J. Dhoble and A. Kumar, *Luminescence*, 2011, **26**, 456.
17 L. Bohaty, P. Becker, H. J. Eichler, J. Hanuza, M. Maczka, K. Takaichi, K. Ueda and A. A. Kaminskii, *Laser Phys.*, 2005, **15**, 1509.
18 A. Silambarasan, P. Rajesh and P. Ramasamy, *J. Cryst. Growth*, 2015, **409**, 95.
19 N. Zaitseva, L. Carman, A. Glenn, J. Newby, M. Faust, S. Hamel, N. Cherepy and S. Payne, *J. Cryst. Growth*, 2011, **314**, 163.
20 X. Luo, S. Pan, X. Fan, J. Wang and G. Liu, *J. Cryst. Growth*, 2009, **311**, 3517.
21 F. Zhang, F. Zhang, J. Qun, S. Pan, Z. Yang and D. Jia, *Phys. Chem. Chem. Phys.*, 2009, **17**, 10489.
22 K. Sankaranarayanan and P. Ramasamy, *J. Cryst. Growth*, 2005, **280**, 467.
23 N. Balamurugan and P. Ramasamy, *Cryst. Growth Des.*, 2006, **6**, 1642.
24 M. Rajalakshmi, T. S. Shyju, R. Indirajith and R. Gopalakrishnan, *Spectrochim. Acta, Part A*, 2012, **86**, 27.
25 A. Silambarasan, P. Rajesh and P. Ramasamy, *AIP Conf. Proc.*, 2015, **1665**, 100012.
26 B. W. Batterman and H. Cole, *Rev. Mod. Phys.*, 1964, **36**, 681.

View Article Online

Published on 16 February 2016. Downloaded by Nanyang Technological University on 15/03/2016 09:34:37.

27 G. Bhagavannarayana, S. Parthiban and S. Meenakshisundaram, *Cryst. Growth Des.*, 2008, **8**, 446.
28 J. Tauc, Optical Properties of Amorphous Semiconductors, in *Amorphous and Liquid Semiconductor*, ed. J. Tauc, Plenum Press, New York, 1974, pp. 170–206.
29 I. P. Bincy and R. Gopalakrishnan, *Opt. Mater.*, 2014, **37**, 267.
30 N. Sivakumar, V. Jayaramakrishnan, K. Baskar and G. Anbalagan, *Opt. Mater.*, 2014, **37**, 780.
31 R. M. Wood, *Laser-Induced Damage of Optical Materials*, Institute of Physics Publishing, Dirac House, Bristol, UK, 2003.
32 H. Yoshida, H. Fujita, M. Nakatsuka, M. Yoshimura1, T. Sasaki1, T. Kamimura and K. Yoshida, *J. Appl. Phys.*, 2006, **45**(2A), 766.
33 B. Milton Boaz, S. M. Navis Priya, J. Mary Linet, P. Martin Devaprasath and S. Jerome Das, *Opt. Mater.*, 2007, **29**, 827.
34 F. Z. Henari, W. J. Blau, L. R. Milgrom, G. Yahioglu, D. Phillips and J. A. Lacey, *Chem. Phys. Lett.*, 1997, **267**, 229.
35 S. Shettigar, G. Umesh, K. Chandrasekharan and B. Kalluraya, *Synth. Met.*, 2007, **157**, 142.
36 M. Sheik-Bahae, A. A. Said, T. Wei, D. J. Hagan and E. W. Van Stryland, *IEEE J. Quantum Electron.*, 1990, **26**, 760.
37 Y. Jiang, L. Miao, G. Jiang, Y. Chen, X. Qi, X. Jiang, H. Zhang and S. Wen, *Sci. Rep.*, 2015, **5**, 16372.
38 Y. S. Zhou, E. B. Wang, J. Peng, J. Liu, C. Hu, R. Huang and X. You, *Polyhedron*, 1999, **18**, 1419.
39 E. W. Van Stryland, Y. Y. Wv, D. J. Hagan, M. J. Soileau and K. Mansour, *J. Opt. Soc. Am. B*, 1988, **5**, 1980.

This journal is © The Royal Society of Chemistry 2016